

1 **A Temperature-Dependent Model for Small-Strain Shear Modulus of Unsaturated Soils**

2

3

4

5

6

7 Farshid Vahedifard, M.ASCE<sup>1</sup>; Sannith Kumar Thota, S.M.ASCE<sup>2</sup>; Toan Duc Cao, A.M.ASCE<sup>3</sup>;

8 Radhavi Abeysiridara Samarakoon, S.M.ASCE<sup>4</sup>; John S. McCartney, F.ASCE<sup>5</sup>

9

10

11

12

*Revised Manuscript Submitted to*

13

*Journal of Geotechnical and Geoenvironmental Engineering (MS GTENG-8804)*

14

15

April 27, 2020

16

17

---

<sup>1</sup> CEE Advisory Board Endowed Professor and Associate Professor, Dept. of Civil and Environmental Engineering, Mississippi State Univ., Mississippi State, MS 39762 (*corresponding author*). Email: farshid@cee.msstate.edu

<sup>2</sup> Graduate Student, Dept. of Civil and Environmental Engineering, Mississippi State Univ., Mississippi State, MS 39762. Email: st1545@msstate.edu

<sup>3</sup> Postdoctoral Associate, Center for Advanced Vehicular Systems (CAVS) and Dept. of Civil and Environmental Engineering, Mississippi State Univ., Mississippi State, MS 39762. Email: toand@cavs.msstate.edu

<sup>4</sup> Graduate Student, Dept. of Structural Engineering, Univ. of California, San Diego, La Jolla, CA 92093. Email: rabey sir@eng.ucsd.edu

<sup>5</sup> Professor and Department Chair, Dept. of Structural Engineering, Univ. of California, San Diego, La Jolla, CA 92093-0085. Email: mccartney@ucsd.edu

18 **ABSTRACT**

19 Near-surface soils in geotechnical and geoenvironmental applications are often unsaturated, and  
20 natural or imposed changes in temperature may lead to a softening effect at constant suction that  
21 causes a change in stiffness. To capture thermal effects on the stiffness of unsaturated soils, this  
22 paper presents an effective stress-based, temperature-dependent model for the small-strain  
23 shear modulus of unsaturated soils, with an emphasis on silts. Temperature dependency of the  
24 model is accounted for by employing temperature-dependent functions for matric suction and  
25 effective saturation characterized using the soil-water retention curve. To validate the proposed  
26 model, laboratory tests using a modified triaxial apparatus with bender elements are carried out  
27 on Bonny silt to measure the small-strain shear modulus at 23 and 43°C for varying matric  
28 suctions of 0 to 110 kPa. The results from the proposed model are in a reasonable agreement  
29 with the experimentally measured values, and demonstrate the importance of considering  
30 temperature effects on the shear modulus of unsaturated soils. The accuracy of the model is  
31 further validated by comparing the predicted values with laboratory test results on silts reported  
32 by two independent studies reported in the literature.

33 **KEYWORDS:**

34 Unsaturated soils; Temperature; Shear modulus; Silt; Stiffness; Suction; Effective stress

35 **INTRODUCTION AND BACKGROUND**

36 Under working stress conditions, geotechnical structures like retaining walls, pavements,  
37 foundations experience shear strains ranging from 0.001% to 1%, with shear strains equal or  
38 smaller than 0.001% representing linear elastic conditions (e.g., Atkinson and Salfors, 1991; Mair  
39 et al., 1993; Atkinson, 2000; Clayton, 2011; Likitlersuang et al., 2013; Ng et al., 2016). The shear  
40 modulus and Young's modulus defined at these small strain magnitudes (also referred to as  
41 elastic moduli) are important soil properties that establish the elastic stress-strain relationships  
42 used extensively in the analysis of geotechnical structures, including immediate settlement of

43 footings and embankments, pavement subgrade deformation response, soil-structure interaction,  
44 and foundation vibration response (e.g., Viggiani and Atkinson, 1995; Kramer, 1996; Rampello et  
45 al., 1997; Likitlersuang et al., 2013; Yang and Gu, 2013). Several experimental studies have  
46 reported that the elastic moduli of soils greatly depend on particle size, void ratio, compaction  
47 energy, matric suction, effective saturation, stress history, and net normal stress (e.g., Hardin and  
48 Black, 1969; Cho and Santamarina, 2001; Mitchell and Soga, 2005; Oh et al., 2009;  
49 Sawangsuriya et al., 2009; Khosravi and McCartney, 2012; Oh and Vanapalli, 2014).

50 Various attempts have been made to experimentally investigate and develop analytical  
51 models for the elastic moduli of unsaturated soils that capture the effects of suction and effective  
52 saturation (e.g., Fredlund et al., 1975; Edil and Motan, 1979; Edil et al., 1981; Mancuso et al.,  
53 2002; Costa et al., 2003; Inci et al., 2003; Khoury and Zaman, 2004; Sawangsuriya et al., 2005;  
54 Khosravi and McCartney, 2012; Dong et al., 2016, 2018). Most of the models developed in these  
55 studies are extensions of models developed for dry or saturated soils by Hardin and his colleagues  
56 (e.g., Hardin and Black, 1969; Hardin, 1978) to unsaturated conditions. Previous studies have  
57 shown that elastic moduli increase with matric suction due to corresponding increases in the  
58 average skeleton stress and stabilization effects of suction on the soil skeleton (e.g., Edil and  
59 Motan, 1979; Mancuso et al., 2002; Costa et al., 2003; Khoury and Zaman, 2004; Sawangsuriya  
60 et al., 2005; Khosravi et al., 2016). An added complication with unsaturated soils is that hydraulic  
61 hysteresis will lead to changes in elastic modulus because of suction-induced hardening  
62 (Khosravi and McCartney, 2012). Another issue is that the shear modulus of soils, in general, will  
63 decrease with the applied shear strain magnitude, and several empirical and semi-empirical  
64 models have been proposed in the literature to establish matric suction-dependent relationships  
65 for shear and Young's moduli of unsaturated soils at larger shear strain magnitudes (e.g.,  
66 Vanapalli et al., 2008; Sawangsuriya et al., 2009; Oh et al., 2009; Lu and Kaya, 2014; Dong et  
67 al., 2018).

68 In many of the geotechnical and geoenvironmental applications mentioned above,  
69 changes in temperature may occur, which have an additional effect on the elastic moduli of  
70 unsaturated soils. Further, other geotechnical applications involving elevated temperatures  
71 include earthen structure-atmospheric interaction under a changing climate, storage of nuclear  
72 waste, energy piles, soil-borehole thermal energy storage systems, buried high voltage cables,  
73 and thermally active earthen structures (e.g., Gens and Olivella, 2001; Laloui and Di Donna, 2013;  
74 Robinson and Vahedifard, 2016; Vahedifard et al., 2015, 2016; 2017; 2018a; McCartney et al.,  
75 2016; Başer et al., 2018; Thota et al., 2019; Shahrokhbadi et al., 2020). Several experimental  
76 studies have illustrated the effects of temperature on the shear strength, volume change and  
77 stiffness of saturated and unsaturated soils (e.g., Cekerevac and Laloui, 2004; Uchaipichat and  
78 Khalili 2009; Coccia et al., 2013; Alsherif and McCartney, 2015; Zhou and Ng, 2016; Ng et al.,  
79 2017). Their studies have provided useful insights through the study of unsaturated constitutive  
80 relationships under at temperatures that rely on different stress state variables (e.g., Bishop's  
81 mean effective stress, matric suction, and deviator stress) and state variables (e.g., specific  
82 volume and effective saturation) for defining temperature-dependent elastic moduli (e.g.,  
83 Cekerevac and Laloui, 2004; Ng et al., 2016; Zhou and Ng, 2017). However, more work is needed  
84 to enhance our understanding of the combined effects of temperature, effective stress state,  
85 anisotropic stress conditions, void ratio, and stress history on the elastic moduli (e.g., McCartney  
86 et al., 2019). Specifically, temperature may affect the soil-water retention curve (SWRC), which  
87 is a key component in the prediction of the effective stress of unsaturated soils (e.g., Lu et al.,  
88 2010). Temperature-induced changes in the SWRC and effective stress can alter the stiffness of  
89 unsaturated soils.

90 Advances in equipment and methodologies for testing unsaturated soils under  
91 temperature-controlled and suction-controlled conditions at various scales have been employed  
92 to gain an improved understanding regarding the effect of temperature on soil stiffness and  
93 underlying mechanisms. However, the impact of temperature on the elastic moduli of unsaturated

94 soils still poses a complex problem, leading to dissimilar trends reported by various investigators.  
95 For example, a group of studies (e.g., Dumont, 2010; Zhou et al., 2015) reported that elastic  
96 moduli decrease with increasing temperature due to reduction of the air-water surface tension.  
97 On the other hand, several studies (e.g., Tanaka et al., 1996; Cekerevac and Laloui, 2004; Laloui  
98 and Cekerevac, 2008) reported that elastic moduli increase with increasing temperature due to  
99 thermal hardening and more interaction between particles. The difference in the reported trends  
100 can possibly be attributed to differences in drainage conditions, mean effective stress and soil  
101 mineralogy (e.g., Uchaipichat, 2005; Uchaipichat and Khalili, 2009; François and Ettahiri, 2012;  
102 Alsherif and McCartney, 2015). For instance, during undrained heating, there may be an increase  
103 in pore-water pressure that leads to a decrease in effective stress and softening, which could  
104 result in decreases in shear modulus. For drained conditions, heating may cause a drying effect  
105 leading to suction hardening, which could result in increase in shear modulus (e.g., McCartney et  
106 al. 2019). The majority of existing thermo-mechanical or thermo-hydro-mechanical constitutive  
107 models for unsaturated soils assume the elastic moduli (including the shear modulus) to be  
108 independent of temperature to simplify formulations (e.g., Thomas and He, 1997; Loret and  
109 Khalili, 2002; Laloui et al., 2003; Bolzon and Schrefler, 2005; Nuth and Laloui, 2008; Zhou and  
110 Ng, 2016). Instead, many thermo-mechanical models assume that the temperature only affects  
111 the mean effective preconsolidation stress (Laloui and Cekerevac 2008). However, results of  
112 several experimental studies (e.g., Cekerevac and Laloui, 2004; Alsherif and McCartney, 2015;  
113 Zhou and Ng, 2016; Ng et al., 2017) suggest that considering temperature-dependent elastic  
114 moduli can lead to more accurate simulations of the mechanical response of unsaturated soils  
115 under elevated temperature.

116 Gaps and unanswered questions remain in the literature regarding the development of  
117 unified models for elastic moduli of unsaturated soils, particularly under elevated temperatures.  
118 Ideally, such models should properly account for all, or the majority of, underlying mechanisms of  
119 through which the temperature affects the elastic response of unsaturated soil under elevated

120 temperatures. To address the aforementioned gaps, this study presents a closed-form  
121 relationship to determine the temperature-dependent small-strain (i.e., 0.001% or lower strain)  
122 shear modulus of unsaturated soils, with an emphasis on silts. For this purpose, a general  
123 functional form is proposed based upon a suction stress-based representation of effective stress  
124 incorporating three primary variables of net normal stress, matric suction, and effective saturation.  
125 Temperature dependency of the model is accounted for by employing temperature-dependent  
126 functions for matric suction and effective saturation characterized using the SWRC. A set of  
127 laboratory tests using a modified triaxial test setup are performed to measure the small-strain  
128 shear modulus of Bonny silt at two different temperatures for varying matric suctions. The  
129 proposed model is validated against the measured data obtained in the current study as well as  
130 those inferred from two other independent experimental studies performed on silts reported in the  
131 literature.

## 132 **THEORY AND FORMULATIONS**

### 133 **General Functional Form**

134 Hardin and Richart (1963) performed a set of micromechanical analyses and showed that the  
135 small-strain shear modulus of soils can be reasonably fitted with an effective stress-dependent  
136 power functional form as follows (Hardin and Richart, 1963):

$$137 \quad G = A_1 f(e) \left[ p' \right]^{n_1} \quad (1)$$

138 where  $A_1$  and  $n_1$  are fitting parameters,  $p'$  is the mean effective stress, and  $f(e)$  is the void ratio  
139 function, which can be expressed for sands and clays as (Hardin, 1978):

$$140 \quad f(e) = \frac{1}{0.3 - 0.7e^2} \quad (2)$$

141 The Hardin and Richart (1963) equation (Eq. 1) is applicable to saturated soils since it is  
142 a function of Terzaghi's effective stress. For unsaturated soils, several studies have built upon

143 Hardin's model and proposed new models for small-strain shear modulus primarily as a function  
 144 of net normal stress and matric suction (e.g., Sawangsuriya et al., 2009; Khosravi and McCartney,  
 145 2009; Khosravi and McCartney, 2012; Ghayoomi et al., 2013; Oh and Vanapalli, 2014; Dong et  
 146 al., 2016). The majority of the previous models (e.g., Mancuso et al., 2002; Mendoza et al., 2005;  
 147 Sawangsuriya et al., 2009; Khosravi and McCartney, 2012; Oh and Vanapalli, 2014) are  
 148 developed using a form of Bishop's effective stress (Bishop, 1959), which is primarily dominated  
 149 by matric suction and effective saturation (Lu et al., 2010). Based on these observations, we  
 150 propose the following general functional form for small-strain shear modulus of unsaturated soils:

$$151 \quad G = A f(e) P_a \left[ \frac{P_n + S_e^{\kappa_{ref}} \psi}{P_a} \right]^n \quad (3)$$

152 where  $P_a$  is the atmospheric pressure used as a normalizing parameter, and  $A$  and  $n$  are fitting  
 153 parameters,  $p_n$  is the mean net normal stress (equal to the difference between the total mean  
 154 stress,  $p$ , and the pore-air pressure,  $u_a$ ),  $S_e$  is the effective saturation, and  $\psi$  is the matric  
 155 suction, which is equal to the difference between the pore-air pressure and the pore-water  
 156 pressure ( $u_w$ ),  $\kappa_{ref}$  is a fitting parameter that controls the impact of variation of water content.  
 157 The effective saturation to the  $\kappa_{ref}$  power is used to represent Bishop's effective stress parameter,  
 158  $\chi$  (Bishop 1959) as suggested by Vanapalli and Fredlund (2000). It should be noted that a similar  
 159 functional form is used by several studies and extensively validated against experimental tests  
 160 performed on various soils at ambient temperature (e.g., Sawangsuriya et al., 2009; Oh and  
 161 Vanapalli, 2014; Dong et al., 2016). The variables used in the proposed functional form represent  
 162 external confining level (by mean net normal stress), soil hardening or softening (by effective  
 163 saturation) and interparticle contact forces (by effective stress) (Dong et al., 2016). The proposed  
 164 function allows to distinctly account for the effect of effective saturation and matric suction, which,

165 while interrelated, are shown to possibly have independent effects on soil hardening or softening  
166 and effective stress (Khalili et al., 2004; Dong et al., 2016).

167 In this study, temperature dependency of the small-strain shear modulus is considered by  
168 incorporating temperature-dependent functions for matric suction and effective saturation, which  
169 is characterized using the SWRC, into the proposed functional form (Eq. 3). Temperature-  
170 dependency of matric suction is accounted for by quantifying the role of temperature on the  
171 surface tension, soil-water contact angle, and adsorption by the enthalpy of immersion. Similar  
172 formulations are employed by Vahedifard et al. (2018b) and Vahedifard et al. (2019) to consider  
173 the effects of temperature on the SWRC and effective stress, respectively.

#### 174 **Temperature-Dependent Matric Suction**

175 The temperature dependency of matric suction, commonly used to represent capillary pressure  
176 in unsaturated soils, is well established in the literature (e.g., Young, 1805; Grant and Salehzadeh,  
177 1996; Lu and Likos, 2004), and arises from changes in the air-water surface tension and the  
178 water-solid contact angle with temperature. For example, the temperature-dependent matric  
179 suction can be defined as (Grant and Salehzadeh, 1996):

$$180 \quad \psi = \psi_{T_r} \left( \frac{\beta + T}{\beta_{T_r} + T_r} \right) \quad (4)$$

181 where  $\psi_{T_r}$  is the matric suction at the reference temperature,  $T$  and  $T_r$  are arbitrary and reference  
182 temperatures, respectively, and  $\beta_{T_r}$  is a regression parameter defined at the reference  
183 temperature  $T_r$ . The parameter  $\beta$  can be estimated as follows (Grant and Salehzadeh, 1996):

$$184 \quad \beta = \frac{-\Delta h T_r}{-\Delta h + a'(\cos \alpha)_{T_r} + b(\cos \alpha)_{T_r} T_r} \quad (5)$$

185 where  $a'$  and  $b$  are fitting parameters that can be estimated from the work of Dorsey (1940) and  
186 Haar et al. (1984) to be  $a' = 0.11766 \text{ Nm}^{-1}$  and  $b = -0.0001535 \text{ Nm}^{-1} \text{ K}^{-1}$ ,  $\alpha$  is the soil-water



187 contact angle, and  $\Delta h$  is the enthalpy of immersion per unit area, which can be determined by  
188 experimental measurements or by using the differential enthalpy of adsorption of the vapor.

189 Grant and Salehzadeh (1996), which is used as the basis of the formulations for  
190 temperature-dependent matric suction in this study, did not consider the effect of temperature on  
191 the enthalpy of immersion. However, previous studies like Watson (1943) demonstrated that  
192 temperature can affect the enthalpy of immersion as well. In this study, we used the following  
193 equation developed by Watson (1943) to account for the reduction of enthalpy with increasing  
194 temperature:

$$195 \quad \Delta h = \Delta h_{T_r} \left( \frac{1-T}{1-T_r} \right)^{0.38} \quad (6)$$

196 where  $\Delta h_{T_r}$  is the enthalpy of immersion per unit area at the reference temperature. Further  
197 discussion about the enthalpy of immersion is presented in the Appendix.

198 The temperature-dependent soil-water contact angle is given as follows (Grant and  
199 Salehzadeh, 1996):

$$200 \quad \cos \alpha = \frac{-\Delta h + TC_1}{a' + bT} \quad (7)$$

201 where  $C_1$  is a constant that can be determined as follows (Grant and Salehzadeh, 1996):

$$202 \quad C_1 = \frac{\Delta h_{T_r} + a'(\cos \alpha)_{T_r} + b(\cos \alpha)_{T_r} T_r}{T_r} \quad (8)$$

203 Considering the Young-Laplace equation, the matric suction (or capillary pressure) is a  
204 function of surface tension and contact angle at a given pore size. These parameters, which  
205 control the matric suction, are sensitive to temperature. Fig. 1 depicts temperature effects on  
206 surface tension, enthalpy of immersion, contact angle, and matric suction at various pore sizes.  
207 As shown in Fig. 1a, the surface tension decreases with an increase in temperature. This could  
208 be due to a reduction in attractive forces because of an increase in molecular thermal sensitivity

209 (e.g., Gardner, 1955; Grant and Bachmann, 2002). Fig 1b depicts the variation of enthalpy of  
210 immersion with temperature for various values of enthalpy of immersion at reference temperature  
211 (see typical enthalpy values for different minerals in Table A1 of Appendix). The temperature-  
212 dependent contact angles are calculated for different enthalpy values and are shown in Fig. 1c.  
213 Based on the proposed model, the enthalpy of immersion (Fig. 1b) and the contact angle (Fig.  
214 1c) increase with temperature. Soils with higher contact angle and enthalpy of immersion are  
215 more sensitive to temperature. The predicted trends of contact angle and enthalpy of immersion  
216 shown in Fig. 1 are consistent with the existing experimental data in the literature (e.g., Watson,  
217 1943; Bachmann et al., 2002; Grant and Bachmann, 2002). Fig. 1d illustrates the variation in  
218 matric suction with temperature for different pore sizes. Typically, a pore size of 0.10 mm  
219 represents fine sand, 0.02 mm represents silt, and 0.0015 mm represents clay (Nimmo, 2004).  
220 For example, at  $r = 0.02$  mm, the matric suction decreases approximately by 18%, 36%, 54%,  
221 and 72% when the soil temperature increases incrementally from 20°C to 40°C, 60°C, 80°C, and  
222 100°C, respectively. The results show the importance of considering temperature effects on the  
223 surface tension, contact angle, and enthalpy of immersion. The predicted thermal effects are  
224 consistent with the trends reported from laboratory tests (Watson, 1943; She and Sleep, 1998;  
225 Bachmann et al., 2002), but are commonly ignored in the majority of existing temperature-  
226 dependent analytical and numerical simulations.

### 227 **Temperature-Dependent Effective Saturation**

228 In this study, we employ the SWRC to characterize the effective saturation. Following the work  
229 by Grant and Salehzadeh (1996), all temperature-dependent SWRC formulations are developed  
230 as a function of matric suction at the reference temperature. Accordingly, Eq. 5 is rearranged to  
231 obtain matric suction at the reference temperature and is incorporated into the SWRC model  
232 proposed by van Genuchten (1980). The temperature-dependent effective saturation can be

233 obtained using the temperature-dependent extension of the van Genuchten SWRC model as  
234 (Vahedifard et al., 2018b):

$$235 \quad S_e = \left( 1 + \left( \alpha_{VG} \psi \left( \frac{\beta_{T_r} + T_r}{\beta + T} \right) \right)^{n_{VG}} \right)^{-m_{VG}} \quad (9)$$

236  
237 where  $\alpha_{VG}$  is a fitting parameter inversely related to the air-entry suction (1/kPa),  $n_{VG}$  is the pore-  
238 size distribution fitting parameter, and  $m_{VG}$  is a fitting parameter representing the overall geometry  
239 of the SWRC assumed to be equal to  $1-1/n_{VG}$ . A key feature of Eq. 10 is that the formulation only  
240 requires the SWRC fitting parameters ( $\alpha_{VG}$  and  $n_{VG}$ ) to be defined at the reference (ambient)  
241 temperature with  $\Delta h_{T_r}$  being the only additional parameter needed to account for the effect of  
242 temperature.

243 Vahedifard et al. (2018b) employed similar formulations for matric suction and effective  
244 saturation to develop temperature-dependent SWRC models. They validated the proposed  
245 formulations versus three laboratory tests on sand, silt, and clay at different temperatures. To  
246 avoid redundancy and keep the focus of this study on shear modulus, we do not repeat the entire  
247 validation results and related discussion for matric suction and SWRC in this paper. For  
248 completeness and using the data presented in Table 1, Fig. 2 shows the predicted effective  
249 saturation from the van Genuchten SWRC model versus measured data for Bonny silt reported  
250 by Alsherif and McCartney (2014, 2015) at temperatures 23°C and 64°C. Results from the  
251 proposed formulation, in general, show good agreement with the measured effective saturation  
252 at different temperatures. Interested readers are referred to Vahedifard et al. (2018b) for further  
253 details regarding validation of the matric suction and effective saturation formulations.

254 To demonstrate the effect of temperature, the extended van Genuchten SWRC model is  
255 used to study the temperature dependency of effective saturation for three silts: Bonny silt  
256 (Alsherif and McCartney, 2015), Bourke silt (Uchaipichat and Khalili, 2009) and a completely

257 decomposed tuff classified as silt (Zhou et al., 2015). Table 1 shows the SWRC parameters used  
258 for determination of temperature-dependent effective saturation for these silts. The SWRC fitting  
259 parameters at ambient temperature are obtained using the measured SWRC data reported by  
260 Alsherif and McCartney (2015), Uchaipichat and Khalili (2009), and Zhou et al. (2015). The  
261 parameter  $\Delta h_{tr}$  is assumed to be the same for all silts and was assumed to be the same as a  
262 silty soil tested by Grant and Salehzadeh (1996).

263 Fig. 3 depicts the changes in the effective saturation at various temperatures ranging from  
264 20°C to 100°C for the three silts. For comparison purposes, the temperature-induced changes in  
265 the effective saturation at matric suction of 150 kPa are examined. For Bonny silt, the effective  
266 saturation decreases by approximately 16%, 28%, 38%, and 55% when increasing the  
267 temperature from 20°C to 40°C, 60°C, 80°C, and 100°C, respectively. For the same temperatures,  
268 the decreases in effective saturation are approximately 13%, 23%, 32% and 49% for Bourke Silt  
269 and 11%, 20%, 28% and 43% for completely decomposed tuff. These decreases in effective  
270 saturation can be due to thermal effects on surface tension, contact angle, and enthalpy  
271 (Vahedifard et al., 2018b). Further, the results for all silts suggest that increasing temperature  
272 leads to a smaller air-entry suction. This finding can contribute to more representative simulations  
273 of unsaturated soils under elevated temperatures. As mentioned before, the proposed  
274 formulations only need the SWRC parameter representing the air entry suction at the reference  
275 temperature. Employing temperature-dependent formulations for the contact angle and enthalpy  
276 of immersion captures the impact of elevated temperature on reducing the air entry suction  
277 (Vahedifard et al., 2019).

### 278 **Closed-Form Equation for Temperature-Dependent Shear Modulus**

279 Using  $S_e$  obtained from the extended van Genuchten SWRC model and by substituting Eqs. (4),  
280 (5), and (10) into Eq. (3), one can obtain the following closed-form model for the temperature-  
281 dependent shear modulus of unsaturated soils:

282

$$G = A f(e) P_a \left\{ \frac{P_n + \left( \left( 1 + \left( \alpha_{VG} \psi \left( \frac{\beta_{T_r} + T_r}{\beta + T} \right) \right)^{n_{VG}} \right)^{-(1-1/n_{VG})} \right)^{\kappa_T} \psi \left( \frac{\beta_{T_r} + T_r}{\beta + T} \right)}{P_a} \right\}^n \quad (10)$$

283 where  $\kappa_T$  is a parameter which controls the impact of effective saturation on the effective stress  
 284 and depends on temperature as follows:

285

$$\kappa_T = \kappa_{ref} + \frac{T - T_r}{T_r} e^{(\kappa_{ref} m)} \quad (11)$$

286 where  $m$  is a fitting parameter equivalent to  $m_{VG}$ . For ambient temperature conditions,  $\kappa_T$   
 287 degenerates to  $\kappa_{ref}$  but the value of  $\kappa_T$  increase as temperature elevates. Physically, Eq. 11  
 288 captures the changes in effective saturation caused by variation of temperature. Heat-induced  
 289 reductions in water content can cause changes in confinement and, therefore, stiffness of the soil  
 290 mass. At a given matric suction, increases in confinement cause sharper reductions in water  
 291 content with temperature. Similar to the proposed temperature-dependent SWRC, all the fitting  
 292 parameters ( $\alpha_{VG}, n_{VG}, n, A, \kappa_{ref}$ ) used in Eq. (11) are those determined at the reference (ambient)  
 293 temperature and  $\Delta h_{T_r}$  is the only additional parameter needed to account for the effect of  
 294 temperature. This feature can facilitate the use of the proposed model as it does not require many  
 295 additional parameters.

296 The proposed formulations for temperature-dependent suction and effective saturation  
 297 can be used to extend other existing models for small-strain shear modulus (e.g., Sawangsuriya  
 298 et al., 2009; Dong et al., 2016) to temperature-dependent conditions. The model presented in this  
 299 study does not consider possible effects of temperature on net normal stress, which may occur  
 300 due to the impact of temperature on pore air pressure. Further, hydraulic hysteresis is not modeled  
 301 but can be considered by following the approach of Khosravi and McCartney (2012). They

302 incorporated the ratio of the mean apparent yield stress to the current mean effective stress (equal  
303 to the overconsolidation ratio, OCR for saturated or dry soils) into the model for the small-strain  
304 shear modulus to consider suction hardening during hydraulic hysteresis.

305 In general, capillarity and adsorption are two main soil-water retention mechanisms (Lu,  
306 2016), which also control the soil stiffness (Lu, 2018). The model proposed in this study is  
307 developed based upon capillarity being the dominant soil-water retention mechanism. This  
308 assumption is legitimate for most soil types including silts, which are the main focus of this study.  
309 For clays, it is prudent to consider both capillarity and adsorption mechanisms in the development  
310 of a shear modulus model. Following this rationale, Lu (2018) proposed a generalized model for  
311 Young's modulus of unsaturated soils at ambient temperature explicitly considering capillarity and  
312 adsorption mechanisms. Temperature can differently affect adsorption and capillarity, an aspect  
313 that needs to be taken into consideration when developing a temperature-dependent model of  
314 small-strain shear modulus including both mechanisms. This can be done by following the  
315 approach outlined by Vahedifard et al. (2018b, 2019) for the development of temperature-  
316 dependent SWRC and effective stress models, respectively.

317 Temperature may affect the small-strain shear modulus through inducing changes in  
318 parameters other than matric suction and effective saturation as well. However, capturing all  
319 relevant temperature-induced mechanisms is certainly not feasible using a closed-form model (as  
320 intended in this study) and warrants employing more complex numerical models. Even with such  
321 numerical models and despite major advances in constitutive modeling of coupled processes in  
322 unsaturated soils, it is still hard to argue that there is a single constitutive model in the literature  
323 than can capture all of the relevant temperature effects. Nevertheless, the proposed model  
324 provides a simple yet reliable tool to account for the temperature effect on the small-strain shear  
325 modulus of unsaturated soils. To the best of the authors' knowledge, this work is the first study  
326 presenting such a closed-form model. Although major elements used in the development of the  
327 proposed model (i.e., temperature-dependent matric suction, SWRC) are already part of the

328 literature, there has been no such an attempt in the literature to make use of all these elements  
329 to develop an analytical model to capture the temperature effect on the shear modulus of  
330 unsaturated soils in the form and details presented in this study.

### 331 **VALIDATION AGAINST EXPERIMENTALLY MEASURED DATA**

332 The accuracy of the proposed model is validated by comparing the predicted values with  
333 experimentally measured results attained from: (a) laboratory tests performed in this study on  
334 Bonny silt using a modified triaxial apparatus with bender elements, and (b) laboratory tests on  
335 silts reported by two independent studies reported in the literature. For each set of data, the  
336 validation process involves two steps: 1) Calibrating the model at ambient temperature to  
337 determine the fitting parameters ( $n$ ,  $A$ , and  $\kappa_{ref}$ ) leading to minimum error using the least square  
338 optimization, and 2) Using the calibrated model to predict the shear modulus at elevated  
339 temperatures and comparing against results from the laboratory tests.

### 340 **Comparison with Laboratory Measurements using Bender Elements**

341 A set of laboratory tests is performed to measure the small strain shear modulus of Bonny silt at  
342 different suctions and temperatures. The tests are carried out using a modified Bishop-Wesley  
343 triaxial apparatus with bender elements. The apparatus is set up to measure shear wave velocities  
344 at different matric suctions for a specific temperature and net normal stress. Fig. 4 shows the  
345 schematic diagram of the complete test setup. Three individual systems are included in the test  
346 setup to measure temperature, matric suction, and shear wave velocities. First, a pressure panel  
347 is used to apply confining, air and water pressures to the specimen. Second, the temperature  
348 controller and circulating pump are used to control and mix the water in the cell to achieve a  
349 desired specimen temperature. In addition, a thermocouple sensor is installed to measure the  
350 temperature in the cell. Third, bender elements are embedded to the top and bottom caps to send  
351 and receive wave signals and therefore measure shear wave velocities.

352 Table 2 displays the index properties of Bonny silt. The specimens used in the tests are  
353 prepared with a thickness of 25 mm and a diameter of 76 mm. The specimen is compacted under  
354 a water content of 10.5% (dry side of optimum) with a void ratio of 0.68 (Alsherif and McCartney,  
355 2015). The compacted specimen is placed in the cell and saturation is achieved by reaching a  
356 minimum B-value of 0.95 at regular intervals of confining and pore water pressures. The axis-  
357 translation technique is used to apply matric suction to the specimen. The air pressure on the top  
358 of the specimen is maintained constant and the water pressure at the bottom is reduced to apply  
359 different matric suction in the specimen. The first matric suction is applied after making sure there  
360 is no change in water levels in the pressure panel for at least 12 hours. The matric suction is  
361 applied in intervals from zero to 110 kPa at two constant temperatures 23°C and 43°C. The next  
362 step of matric suction is applied after the specimen reaches a steady or equilibrium state. For  
363 both tests, the specimens were confined at a constant net normal stress of ~ 50 kPa. To assess  
364 the variability of results, multiple wave velocity measurements are made at a given suction after  
365 reaching suction equilibrium. The measurements are found to be identical implying zero  
366 variability. The suction is increased to the next level only after the wave velocities remain constant  
367 for at least 12 hours.

368 The measured shear wave velocities at different matric suctions and temperatures  
369 obtained from the experimental tests are used to determine the small-strain shear modulus as:

$$370 \quad G = \rho V^2 \quad (12)$$

371 where  $\rho$  is the total density of the soil and  $V$  is the shear wave velocity of the soil.

372 Fig. 5 depicts the measured and predicted small-strain shear modulus versus matric  
373 suction at  $T = 23^\circ\text{C}$  and  $T = 43^\circ\text{C}$ . The experimentally measured data demonstrate that the shear  
374 wave velocities, and therefore the small-strain shear modulus, are affected by matric suction and  
375 temperature. At a given temperature, the shear modulus increases with an increase in matric  
376 suction. At a given matric suction, the shear modulus decreases with an increase in temperature.



377 The effect of temperature on shear modulus is more pronounced in higher matric suctions. For  
378 example, at matric suction of 40 kPa, the reduction of shear modulus is approximately 16% by  
379 increasing temperature from 23 to 43°C. At higher matric suction of 100 kPa, the reduction of  
380 shear modulus is approximately 39% by increasing temperature from 23 to 43°C. This could be  
381 due to variation in effective stress and in turn the stiffness at a higher temperature depending on  
382 the range of matric suction. At low range of matric suction, the trend of effective stress with  
383 temperature is similar to the one shown in Vahedifard et al. (2019). For the proposed model, the  
384 input parameters  $A = 1000$ ,  $n = 2.1$ ,  $\alpha_{VG} = 0.05 \text{ kPa}^{-1}$ ,  $n_{VG} = 2.2$ ,  $\kappa_{ref} = 0.35$ ,  $\Delta h_{Tr} = -0.516 \text{ Jm}^{-2}$   
385 are used to calibrate and predict the shear modulus at ambient and elevated temperatures. The  
386 root mean square error (RMSE) values of the model with respect to the measured data are 22  
387 MPa and 22 MPa at 23°C and 43°C, respectively. As seen, the model shows a reasonable match  
388 with the measured values for the elevated temperature case ( $T = 43^\circ\text{C}$ ). The only exception where  
389 the model shows a relatively high over estimation is at matric suction of 75 kPa and  $T = 23^\circ\text{C}$ .  
390 The large difference can be possibly due to the measured shear modulus being somehow lower  
391 than expected at this point, which can be due to testing issues and limitations.

### 392 **Comparison with Experimental Data Reported in the Literature**

393 There is no experimental data in the literature directly reporting the small-strain shear modulus of  
394 unsaturated soils under elevated temperatures. Nevertheless, data from tests at higher shear  
395 strain amplitudes are used to extrapolate trends in the small-strain shear modulus available data  
396 in the literature for further validation of the proposed model. For this purpose, we use results from  
397 suction-controlled temperature-controlled triaxial tests on Bourke silt (reported by Uchaipichat and  
398 Khalili, 2009) and completely decomposed tuff (reported by Zhou et al., 2015). Following the  
399 procedure explained below, we infer the shear modulus of the tested soils at a shear strain of  
400 0.001% and use for validation against predictions of the proposed model. Table 3 presents a

401 summary of the experimental testing matrix used for calibration and validation purposes in this  
 402 section.

403 For the results presented by Uchaipichat and Khalili (2009), the finite-strain Young's  
 404 modulus at an axial strain of 1% is obtained from the reported deviatoric stress-axial strain curve  
 405 for each tested combination of net normal stress, temperature, and suction. The corresponding  
 406 finite-strain shear modulus is calculated using a Poisson's ratio of 0.25 (e.g., Alsharif and  
 407 McCartney, 2015), and is then scaled to 0.001% strain using the scaling equation proposed by  
 408 Dong et al. (2018) as follows:

$$409 \quad \frac{G^*}{G} = \frac{1}{1 + \left[ \frac{\gamma}{\alpha_{VG}(p_n + S_e \psi) \gamma_{ref}} \right]} \quad (13)$$

410 where  $G^*$  is the finite-strain modulus,  $\gamma_{ref}$  is the reference shear strain. The reference shear  
 411 strain can be defined as (Dong et al., 2018):

$$413 \quad \gamma_{ref} = \eta \theta^\xi \quad (14)$$

414 where  $\eta$  is a multiplier parameter,  $\xi$  is the power factor for water content,  $\theta$  is the volumetric  
 415 water content, which is related to  $S_e$  as follows:

$$417 \quad S_e = \frac{\theta - \theta_r}{\theta_s - \theta_r} \quad (15)$$

418 where  $\theta_s$  and  $\theta_r$  are the saturated and residual volumetric water contents, respectively. For the  
 419 data reported by Uchaipichat and Khalili (2009), the following parameters are used to scale the  
 420 measured finite-strain shear moduli to small-strain conditions:  $\theta_r = 0.1258$ ,  $\theta_s = 0.55$ ,  $\gamma = 1\%$ ,  
 421  $\eta = 0.0027$ , and  $\xi = 1.857$ .

422 Zhou et al. (2015) reported the measured secant shear modulus at several shear strains  
 423 ranging from 0.003% to 1%. Using regression analysis to find the best nonlinear fit passing  
 424 through the data, we employ the regression equation to infer the shear modulus at 0.001% strain,

425  $G_{0.001}$ . Fig. 6 shows the measured shear moduli versus shear strain for the tested silt reported by  
426 Zhou et al. (2015) and best-fit curves through the measured data.

427 For calibration, the SWRC parameters given in Table 1 are used in the model. Table 4  
428 summarizes the calibrated fitting parameters of the proposed shear modulus model at ambient  
429 temperature for the two silts. Fig. 7 provides a comparison between the inferred shear moduli at  
430 0.001% strain ( $G_{0.001}$ ) against calibrated results at ambient temperature and predicted results at  
431 elevated temperatures. For both Bourke silt and the decomposed tuff, the results of the proposed  
432 model are in good agreement with the experimental data. It is noted that more tests at higher  
433 matric suctions are needed to better understand and model the shear stiffness of unsaturated  
434 soils at high matric suctions under elevated temperature.

## 435 **CONCLUSIONS**

436 Capturing the temperature dependency of small-strain shear modulus can be an important aspect  
437 of modeling the behavior of unsaturated soils subjected to varying temperatures. This study  
438 presented a closed-form model to determine the temperature-dependent small-strain shear  
439 modulus of unsaturated soils, with an emphasis on silts. An effective stress-based general  
440 functional form was proposed, and temperature dependency of the model was considered by  
441 incorporating temperature-dependent functions for matric suction and effective saturation. The  
442 effective saturation was presented by analytical expressions in which the effects of temperature  
443 were considered on the surface tension, soil-water contact angle, and adsorption by the enthalpy  
444 of immersion per unit area. The proposed formulations were used to extend the SWRC model  
445 originally developed by van Genuchten (1980), which was then used to develop the equations for  
446 temperature-dependent shear modulus of unsaturated soils at small strains. Further, a series of  
447 experimental tests were conducted to measure the small-strain shear modulus of unsaturated  
448 Bonny silts at elevated temperatures. The proposed formulation was compared and validated

449 against the experimental data from the current study and two other independent studies reported  
450 the literature. The results of the proposed model showed good match against the measured data.

451 The model presented in this study can contribute toward an improved understanding of  
452 the temperature effect on the mechanical response of unsaturated soils. Experimental  
453 measurements of elastic moduli of unsaturated soils under different temperatures require time-  
454 consuming tests and certain expertise. Hence, empirical or semi-empirical models such as that  
455 developed in this study can facilitate the implementation of temperature-dependent analyses in  
456 the geotechnical engineering practice by providing a reasonable estimation of the small-strain  
457 shear modulus of unsaturated soils at elevated temperatures. The proposed formulation offers a  
458 generalized model and involves constitutive relationships that are needed in a coupled heat  
459 transfer and water flow model. As the degree of saturation, suction, and temperature changes  
460 during a transient flow process, the model should still provide accurate predictions. Thus, the  
461 model can be incorporated as a constitutive relationship into both steady-state and transient flow  
462 and heat analyses. This study is the first attempt in the literature to experimentally measure and  
463 predict the small-strain shear modulus of unsaturated soils at elevated temperatures. For future  
464 studies, more experimental tests are recommended to examine and further validate the proposed  
465 model for different soil types and wider ranges of suction and temperature.

#### 466 **ACKNOWLEDGMENTS**

467 This material is based upon work supported in part by the National Science Foundation under  
468 Grant No. CMMI-1634748. Any opinions, findings, and conclusions or recommendations  
469 expressed in this material are those of the authors and do not necessarily reflect the views of the  
470 National Science Foundation.

#### 471 **APPENDIX: ENTHALPY OF IMMERSION AT REFERENCE TEMPERATURE**

472 The enthalpy of immersion at the reference temperature ( $\Delta h_{T_r}$ ) is a key input parameter in the  
473 proposed formulations and is defined by the International Union of Pure and Applied Chemistry

474 (IUPAC) as the difference between the enthalpy of a solid completely immersed in a wetting fluid  
475 and that of the solid and the liquid taken separately (Grant and Salehzadeh, 1996). The value of  
476  $\Delta h_{T_r}$  must be specified whether the solid in the initial state is in contact with vacuum or with the  
477 vapor of the liquid at a given partial pressure. According to Everett (1972), the measurements of  
478 the enthalpy of wetting of a solid equilibrated with varying relative pressures of the vapor of a pure  
479 wetting liquid may be used to derive the differential enthalpy of adsorption. Jaroniec and Madey  
480 (1988) showed that the enthalpy of immersion is proportional to the average adsorption potential  
481 and can be calculated using the parameters characterizing the energetic heterogeneity of  
482 microporous solids. Table A1 presents  $\Delta h_{T_r}$  of different materials reported in the literature.

483 The enthalpy of immersion at the reference temperature can be determined based on  
484 experimentally measured variables. For example, as per Harkins and Jura (1944),  $\Delta h_{T_r}$  can be  
485 calculated as:

$$486 \Delta h_{T_r} = -[\sigma(\cos \alpha)]_{T_r} \quad (16)$$

488 where  $\sigma$  is the air-water surface tension at  $T_r$ . There are several studies in the literature that  
489 experimentally measure  $\sigma$  and  $\cos \alpha$  (e.g., She and Sleep, 1998; Bachmann et al., 2002).  
490 Further, previous studies have proposed several empirical models for  $\Delta h_{T_r}$  (e.g., Stoeckli and  
491 Kraehenbuehl, 1981; Watson, 1943; Kahr et al., 1990). Kahr et al. (1990) proposed the following  
492 expression for the enthalpy of immersion of sodium and calcium bentonites as a function of initial  
493 total water content ( $\theta$ ) at the reference temperature of 293 K:

$$494 \Delta h_{T_r} = A \exp(-B\theta - C\theta^2) \quad (17)$$

495 where  $A$ ,  $B$ , and  $C$  are fitting parameters.

#### 496 **DATA AVAILABILITY STATEMENT**

497 All data, models, and code generated or used during the study appear in the submitted article.

498 **REFERENCES**

- 499 Alsherif, N. A., and McCartney, J. S. (2014). "Effective stress in unsaturated silt at low degrees of  
500 saturation." *Vadose Zone Journal*, 13(5).
- 501 Alsherif, N. A., and McCartney, J. S. (2015). "Thermal behaviour of unsaturated silt at high suction  
502 magnitudes." *Géotechnique*, 65(9), 703-716.
- 503 Atkinson, J. H., and Sallfors, G. (1991). Experimental determination of soil properties (stress-  
504 strain-time). *In Proc. 10th Eur. Conf: Soil Mech.*, Florence, 3, 915.
- 505 Atkinson, J. H. (2000). "Non-linear soil stiffness in routine design." *Géotechnique*, 50(5), 487-508.
- 506 Bachmann, J., Horton, R., Grant, S. A., and Van der Ploeg, R. R. (2002). "Temperature  
507 dependence of water retention curves for wettable and water-repellent soils." *Soil Sci. Soc.*  
508 *Am. J.*, 66(1), 44-52.
- 509 Başer, T., Dong, Y., Moradi, A.M., Lu, N., Smits, K., Ge, S., Tartakovsky, D. and McCartney, J.S.,  
510 (2018). "Role of Nonequilibrium Water Vapor Diffusion in Thermal Energy Storage  
511 Systems in the Vadose Zone." *J. Geotech. Geoenviron. Eng.*, 144(7), 04018038.
- 512 Bishop, A. W. (1959). "The principle of effective stress." *Tecnisk Ukeblad*, 106(39), 859–863.
- 513 Bolzon, G., and Schrefler, B. A. (2005). "Thermal effects in partially saturated soils: a constitutive  
514 model." *Int. J. Numer. Anal. Methods Geomech.*, 29(9), 861-877.
- 515 Brooks, C. S. (1960). "Free energies of immersion for clay minerals in water, ethanol and n-  
516 heptane." *The Journal of Physical Chemistry*, 64(5), 532-537.
- 517 Cekerevac, C., and Laloui, L. (2004). "Experimental study of thermal effects on the mechanical  
518 behaviour of a clay." *Int. J. Numer. Anal. Methods Geomech.*, 28(3), 209-228.
- 519 Cho, G. C., and Santamarina, J. C. (2001). "Unsaturated particulate materials-particle-level  
520 studies." *J. Geotech. Geoenviron. Eng.*, 127(1), 84-96.
- 521 Clayton, C. R. I. (2011). "Stiffness at small strain: research and practice." *Géotechnique*, 61(1),  
522 5-37.

523 Coccia, C. J. R., Casady, A., and McCartney, J. S. (2013). "Physical modeling of the mechanical  
524 improvement of unsaturated silt through heating." *Proceedings of the 1st Pan-American*  
525 *Conference on Unsaturated Soils*. Feb. 20-22. Cartagena de Indias. Taylor and Francis  
526 Group, London. pp. 141-146.

527 Costa, Y. D., Cintra, J. C., and Zornberg, J. G. (2003). "Influence of matric suction on the results  
528 of plate load tests performed on a lateritic soil deposit." *Geotech. Test. J.*, 26(2), 1-9.

529 Dong, Y., Lu, N., and McCartney, J.S. (2016). "A unified model for small-strain shear modulus of  
530 variably saturated soil." *J. Geotech. Geoenviron. Eng.*, 142(9), 04016039.

531 Dong, Y., Lu, N., and McCartney, J.S. (2018). "Scaling shear modulus from small to finite strain  
532 for variably saturated soils." *J. Geotech. Geoenviron. Eng.*, 144(2), 04017110.

533 Dorsey, N. E. (1940). Properties of ordinary water substance. Reinhold, New York.

534 Dumont, E. R. (2010). "Bone density and the lightweight skeletons of birds." Proceedings of the  
535 Royal Society of London B: Biological Sciences, rspb20100117.

536 Grant, S. A., and Bachmann, J. (2002). Effect of temperature on capillary pressure. *Geophysical*  
537 *Monograph-American Geophysical Union*, 129, 199-212.

538 Edil, T. B., and Motan, S. E. (1979). "Soil-water potential and resilient behavior of subgrade  
539 soils." *Transportation Research Record*, (705).

540 Edil, T. B., Motan, S. E., and Toha, F. X. (1981). "Mechanical behavior and testing methods of  
541 unsaturated soils." *Laboratory Shear Strength of Soil*, ASTM STP 740, ASTM, West  
542 Conshohoken, Pa.

543 Everett, D. H. (1972). "Definitions terminology and symbols in colloid and surface chemistry."  
544 *Pure Appl. Chem.*, 31(4), 579-638.

545 François, B., and Ettahiri, S. (2012). Role of the soil mineralogy on the temperature dependence  
546 of the water retention curve. In *Unsaturated soils: Research and applications* (pp. 173-  
547 178). Springer, Berlin, Heidelberg.

548 Fredlund, D. G., Bergan, A. T., and Sauer, E. K. (1975). "Deformation characterization of  
549 subgrade soils for highways and runways in northern environments." *Can. Geotec.*  
550 *J.*, 12(2), 213-223.

551 Gens, A., and Olivella, S. (2001). "Clay barriers in radioactive waste disposal." *Revue française*  
552 *de génie civil*, 5(6), 845-856.

553 Ghayoomi, M., McCartney, J. S., and Ko, H. Y. (2013). "Empirical methodology to estimate  
554 seismically induced settlement of partially saturated sand." *J. Geotech. Geoenviron. Eng.*,  
555 139(3), 367-376.

556 Grant, S. A., and Salehzadeh, A. (1996). "Calculation of temperature effects on wetting  
557 coefficients of porous solids and their capillary pressure functions." *Water Resour. Res.*,  
558 32 (2), 261-270.

559 Haar, L., Gallagher, J. S., and Kell, G. S. (1984). "NBS/NRC Steam Table." Hemisphere Publ.  
560 Corp, New York.

561 Hardin, B. O., and Black, W. (1969). "Closure on vibration modulus of normally consolidated  
562 clay." *J. of Soil Mech. and Found. Div.*, 95(6), 1531-1537.

563 Hardin, B. O. (1978). "The nature of stress-strain behavior of soils." *Proc., of the Geotechnical*  
564 *Engineering Division Specialty Conf. on Earthquake Engineering and Soil Dynamics*,  
565 ASCE, New York, 1, 1-90.

566 Hardin, B. O., and Richart Jr, F. E. (1963). "Elastic wave velocities in granular soils." *J. of Soil*  
567 *Mech. and Found. Div.*, 33-65.

568 Harkins, W. D., and Jura, G. (1944). "Surfaces of solids. XII. An absolute method for the  
569 determination of the area of a finely divided crystalline solid." *Journal of the American*  
570 *Chemical Society*, 66(8), 1362-1366.

571 Inci, G., Yesiller, N., and Kagawa, T. (2003). "Experimental investigation of dynamic response of  
572 compacted clayey soils." *Geotech. Test. J.*, 26(2), 125-141.



573 Jaroniec, M., and Madey, R. (1988). Enthalpy of immersion of a microporous solid. *The Journal*  
574 *of Physical Chemistry*, 92(13), 3986-3988.

575 Kahr, G., Kraehenbuehl, F., Stoeckli, H. F., and Müller-Vonmoos, M. (1990). "Study of the water-  
576 bentonite system by vapour adsorption, immersion calorimetry and X-ray techniques; II,  
577 Heats of immersion, swelling pressures and thermodynamic properties." *Clay Minerals*,  
578 25(4), 499-506.

579 Khalil, A. M. (1978). "Thermal treatment of nonporous silica, 1, Chemistry of the surface and heats  
580 of immersion in water." *J. Colloid Interface Sci.*, 66, 509-515.

581 Khalili, N., Geiser, F., and Blight, G. E. (2004). "Effective stress in unsaturated soils: Review with  
582 new evidence." *Int. J. Geomech.*, 4(2), 115–126.

583 Khosravi, A., and McCartney, J. S. (2009). "Impact of stress state on the dynamic shear moduli  
584 of unsaturated, compacted soils." *Proc., 4th Asia Pacific Conf. Unsat. Soils*, O. Buzzi, S.  
585 Fityus, and D. Sheng, eds., Construction Research Council Press/Balkema, Newcastle,  
586 Australia, 1–6.

587 Khosravi, A., and McCartney, J. S. (2012). "Impact of hydraulic hysteresis on the small-strain  
588 shear modulus of low plasticity soils." *J. Geotech. Geoenviron. Eng.*, 138(11), 1326-1333.

589 Khosravi, A., Salam, S., McCartney, J. S. and Dadashi, A., (2016). "Suction-induced hardening  
590 effects on the shear modulus of unsaturated silt." *International Journal of*  
591 *Geomechanics*, 16(6), D4016007.

592 Khoury, N. N., and Zaman, M. M. (2004). "Correlation between resilient modulus, moisture  
593 variation, soil suction for subgrade soils." *Transportation Research Record*, 1874,  
594 Transportation Research Board, Washington, D.C.

595 Kramer, S. L. (1996). *Geotechnical earthquake engineering*. In prentice-Hall international series  
596 in civil engineering and engineering mechanics. Prentice-Hall, New Jersey.

597 Laloui, L., Klubertanz, G., and Vulliet, L. (2003). "Solid-liquid-air coupling in multiphase porous  
598 media." *Int. J. Numer. Anal. Methods Geomech.*, 27(3), 183-206

599 Laloui, L., and Cekerevac, C. (2008). "Numerical simulation of the non-isothermal mechanical  
600 behaviour of soils." *Computers and Geotechnics*, 35(5), 729-745.

601 Laloui, L., and Di Donna, A. (2013). *Energy geostructures: innovation in underground*  
602 *engineering*. John Wiley and Sons.

603 Loret, B., and Khalili, N. (2002). "An effective stress elastic-plastic model for unsaturated porous  
604 media." *Mechanics of Materials*, 34(2), 97-116.

605 Likitlersuang, S., Teachavorasinskun, S., Surarak, C., Oh, E., and Balasubramaniam, A. (2013).  
606 "Small strain stiffness and stiffness degradation curve of Bangkok clays." *Soils and*  
607 *Foundations*, 53(4), 498-509.

608 Lu, N. (2016). "Generalized soil water retention equation for adsorption and capillarity." *J.*  
609 *Geotech. Geoenviron. Eng.*, 142(10), 04016051.

610 Lu, N., (2018). "Generalized elastic modulus equation for unsaturated soil." *Proc. PanAm*  
611 *Unsaturated Soils 2017: Plenary Papers*, L. R. Hoyos et al. (Eds), Second Pan-American  
612 Conference on Unsaturated Soils: Unsaturated Soil Mechanics for Sustainable  
613 Geotechnics, Geotechnical Special Publication No. 300, November 12-15, 2017, Dallas,  
614 TX, ASCE, Reston, VA, 32-48, DOI: 10.1061/9780784481677.002.

615 Lu, N., and W. J. Likos. (2004). *Unsaturated Soil Mechanics*. Hoboken, NJ: Wiley.

616 Lu, N., and Likos, W. J. (2006). "Suction stress characteristic curve for unsaturated soil." *J.*  
617 *Geotech. Geoenviron. Eng.*, 132(2), 131-142.

618 Lu, N., Godt, J. W., and Wu, D. T. (2010). "A closed-form equation for effective stress in  
619 unsaturated soil." *Water Resour. Res.*, 46(5), W05515.

620 Lu, N., and Kaya, M. (2014). "Power law for elastic moduli of unsaturated soil." *J. Geotech.*  
621 *Geoenviron. Eng.*, 140(1), 46-56.

622 Mair, R. J., Taylor, R. N., and Bracegirdle, A. (1993). "Subsurface settlement profiles above  
623 tunnels in clays." *Géotechnique*, 43(2), 315-320.

624 Mancuso, C., Vassallo, R., and d’Onofrio, A. (2002). “Small strain behavior of a silty sand in  
625 controlled-suction resonant column-torsional shear tests.” *Can. Geotech. J.*, 39(1), 22–31.

626 Mendoza, C. E., Colmenares, J. E., and Merchan, V. E. (2005). “Stiffness of an unsaturated  
627 compacted clayey soil at very small strains.” *In Proc., Advanced Experimental*  
628 *Unsaturated Soil Mechanics: Proceedings of the International Symposium on Advanced*  
629 *Experimental Unsaturated Soil Mechanics*, Trento, Italy, 27-29 June 2005, Taylor &  
630 Francis Group, London, 199-204.

631 McCartney, J. S., Sánchez, M., and Tomac, I. (2016). “Energy geotechnics: Advances in  
632 subsurface energy recovery, storage, exchange, and waste management.” *Computers*  
633 *and Geotechnics*, 75, 244-256.

634 McCartney, J. S., Jafari, N. H., Hueckel, T., Sanchez, M., Vahedifard, F. (2019). “Thermal energy  
635 issues in geotechnical engineering.” *Geotechnical Fundamentals for Addressing New*  
636 *World Challenges*. N. Lu and J.K. Mitchell, Eds. Springer. 275-317, DOI:  
637 [https://doi.org/10.1007/978-3-030-06249-1\\_10](https://doi.org/10.1007/978-3-030-06249-1_10).

638 Mitchell, J. K., and Soga, K. (2005). *Fundamentals of Soil Behavior*, New York: John Wiley and  
639 Sons.

640 Mon, E. E., Hamamoto, S., Kawamoto, K., Komatsu, T., and Møldrup, P. (2013). “Temperature  
641 effects on geotechnical properties of kaolin clay: simultaneous measurements of  
642 consolidation characteristics, shear stiffness, and permeability using a modified  
643 oedometer.” *GSTF Journal of Geological Sciences (JGS)*, 1(1).

644 Ng, C. W. W., and Zhou, C. (2014). “Cyclic behaviour of an unsaturated silt at various suctions  
645 and temperatures.” *Géotechnique*, 64(9), 709-720.

646 Ng, C. W. W., Zhou, C., and Xu, J. (2016). “Monotonic and Cyclic Shear Stiffness of Unsaturated  
647 Soil at Different Temperatures.” *Unsaturated Soil Mechanics from Theory to Practice-*  
648 *Proceedings of the 6th Asia-Pacific Conference on Unsaturated Soils*, 89-101.

649 Ng, C. W. W., Mu, Q. Y., and Zhou, C. (2017). "Effects of soil structure on the shear behaviour of  
650 an unsaturated loess at different suctions and temperatures." *Can. Geotech. J.*, 54(2),  
651 270-279.

652 Nimmo, J. R. (2004). "Porosity and pore size distribution." In Vol. 3 of *Encyclopedia of soils in the*  
653 *environment*, edited by D. Hillel, 295–303. London: Elsevier.

654 Nuth, M., and Laloui, L. (2008). "Effective stress concept in unsaturated soils: clarification and  
655 validation of a unified framework." *J. Numer. Anal. Methods Geomech.*, 32(7), 771-801.

656 Oh, W. T., Vanapalli, S. K., and Puppala, A. J. (2009). "Semi-empirical model for the prediction of  
657 modulus of elasticity for unsaturated soils." *Can. Geotech. J.*, 46(8), 903-914.

658 Oh, W. T., and Vanapalli, S. K. (2014). "Semi-empirical model for estimating the small-strain shear  
659 modulus of unsaturated non-plastic sandy soils." *Geotechnical and Geological*  
660 *Engineering*, 32(2), 259-271.

661 Partyka, S., Rouquerol, F., and Rouquerol, J. (1979). "Calorimetric determination of surface  
662 areas, Possibilities of a modified Harkins and Jura procedure." *J. Colloid Interface Sci.*,  
663 68, 21-31.

664 Rampello, S., Viggiani, G. M. B., and Amorosi, A. (1997). "Small-strain stiffness of reconstituted  
665 clay compressed along constant triaxial effective stress ratio paths." *Géotechnique*, 47(3),  
666 475-489.

667 Robinson, J. D., and Vahedifard, F. (2016). "Weakening mechanisms imposed on California's  
668 levees under multiyear extreme drought." *Climatic change*, 137(1-2), 1-14.

669 Sawangsuriya, A., Edil, T. B., and Bosscher, P. J. (2009). "Modulus-suction-moisture relationship  
670 for compacted soils in postcompaction state." *J. Geotech. Geoenviron. Eng.*, 135(10),  
671 1390-1403.

672 Sawangsuriya, A., Edil, T. B., and Bosscher, P. J. (2005). "Stiffness behavior of an unsaturated  
673 pavement subgrade soil." Proc., of Int. Conf. on Problematic Soils, Eastern Mediterranean  
674 University Press, Famagusta, N. Cyprus, 209–217.

675 Shahrokhbadi, S, Cao, T. C., and Vahedifard, F. (2020). "Thermo-Hydro-Mechanical Modeling  
676 of Unsaturated Soils using Isogeometric Analysis: Model Development and Application to  
677 Strain Localization Simulation." *International Journal for Numerical and Analytical*  
678 *Methods in Geomechanics*, 44(2), 261-292

679 She, H. Y., and Sleep, B. E. (1998). "The effect of temperature on capillary pressure-saturation  
680 relationships for air-water and perchloroethylene-water systems." *Water Resour. Res.*,  
681 34(10), 2587-2597.

682 Stoeckei, H. F., and Kraehenbuehl, F. (1981). "The enthalpies of immersion of active carbons in  
683 relation to the Dubinin theory for the volume filling of micropores." *Carbon*, 19, 353-356.

684 Tanaka, K., Okamoto, K., Inui, H., Minonishi, Y., Yamaguchi, M., and Koiwa, M. (1996). "Elastic  
685 constants and their temperature dependence for the intermetallic compound  
686 Ti<sub>3</sub>Al." *Philosophical Magazine A*, 73(5), 1475-1488.

687 Thomas, H. R., and He, Y. (1997). "A coupled heat-moisture transfer theory for deformable  
688 unsaturated soil and its algorithmic implementation." *Int. J. Numer. Meth. Eng.*, 40(18),  
689 3421-3441.

690 Thota, S. K., Cao, T. C., Vahedifard, F., and Ghazanfari, E. (2019). "Stability Analysis of  
691 Unsaturated Slopes under Nonisothermal Conditions." *Proc. Geo-Congress 2019, Eighth*  
692 *International Conference on Case Histories in Geotechnical Engineering*, Geotechnical  
693 Special Publication No. 310. Philadelphia, PA, March 24-27, ASCE, Reston, VA, 844-852,  
694 DOI: 10.1061/9780784482124.085.

695 Uchaipichat, A., and Khalili, N. (2009). "Experimental investigation of thermo-hydro-mechanical  
696 behaviour of an unsaturated silt." *Géotechnique*, 59(4), 339-353.

697 Vahedifard, F., AghaKouchak, A., and Robinson, J. D., (2015). "Drought Threatens California's  
698 Levees." *Science*, 349(6250), 799.

699 Vahedifard, F., Robinson, J. D., and AghaKouchak, A. (2016). "Can Protracted Drought  
700 Undermine the Structural Integrity of California's Earthen Levees?" *J. Geotech.*  
701 *Geoenviron. Eng.*, 142(6), 02516001.

702 Vahedifard, F., AghaKouchak, A., Ragno, E., Shahrokhbadi, S., and Mallakpour, I., (2017).  
703 "Lessons from the Oroville Dam." *Science*, 355(6330), 1139-1140.

704 Vahedifard, F., Williams, J. M., and AghaKouchak, A. (2018a). "Geotechnical Engineering in the  
705 Face of Climate Change: Role of Multi-Physics Processes in Partially Saturated Soils." In  
706 Proc. IFCEE 2018, GSP No. 295, 353-364.

707 Vahedifard, F., Cao, T. D., Thota, S. K., and Ghazanfari, E. (2018b). "Nonisothermal Models for  
708 Soil–Water Retention Curve." *J. Geotech. Geoenviron. Eng.*, 144(9), 04018061.

709 Vahedifard, F., Cao, T. C., Ghazanfari, E., and Thota, S. K., (2019). "Closed-Form Models for  
710 Nonisothermal Effective Stress of Unsaturated Soils." *J. Geotech. Geoenviron. Eng.*,  
711 145(9), 04019053.

712 Vanapalli, S.K., Oh, W. T. and Puppala, A. J. (2008). "A simple model for predicting modulus of  
713 elasticity of unsaturated sandy soils." In Toll et al. (ed.), *Unsaturated soils: Advances in*  
714 *Geo-engineering*, 503-509. Rotterdam: Balkema.

715 van Genuchten, M. T. (1980). "A closed-form equation for predicting the hydraulic conductivity of  
716 unsaturated soils." *Soil Sci. Soc. Am. J.*, 44(5), 892–898.

717 Viggiani, G., and Atkinson, J. H. (1995). "Interpretation of bender element tests."  
718 *Géotechnique*, 45(1), 35-53.

719 Watson, K. M. (1943). "Thermodynamics of the liquid state." *Ind. Eng. Chem.*, 35 (4), 398–406.

720 Whalen, J. W. (1961). "Thermodynamic properties of water adsorbed on quartz." *J. Phys. Chem.*,  
721 65, 1676-1681.

722 Yang, J., and Gu, X. (2013). "Shear stiffness of granular material at small strains: Does it depend  
723 on grain size?." *Géotechnique*. 63(2), 165-179.

724 Young, T. (1805). "An essay on the cohesion of fluids." *Philos. Trans. R. Soc.*, 95, 65–87.

725 Zettlemoyer, A. C., Young, G. J., & Chessick, J. J. (1955). "Studies of the Surface Chemistry of  
726 Silicate Minerals. III. Heats of Immersion of Bentonite in Water." *The Journal of Physical*  
727 *Chemistry*, 59(9), 962-966.

728 Zhou, C., and Ng, C. W. W. (2016). "Effects of temperature and suction on plastic deformation of  
729 unsaturated silt under cyclic loads." *Journal of Materials in Civil Engineering*, 28(12),  
730 04016170.

731 Zhou, C., and Ng, C. W. W. (2017). "Constitutive modelling of shear stiffness degradation at  
732 various suctions and temperatures." Proceedings of the 19<sup>th</sup> International Conference on  
733 Soil Mechanics and Geotechnical Engineering, Seoul, 2077-2080.

734 Zhou, C., Xu, J., and Ng, C. W. W. (2015). "Effects of temperature and suction on secant shear  
735 modulus of unsaturated soil." *Géotechnique Letters*, 5(3), 123-128.

736

737

738

739

740

741  
742

**Table 1.** SWRC parameters used for calculating temperature-dependent effective saturation

Soil Type	$\Delta h_{T_r}$ (Jm <sup>-2</sup> )	$T_r$ (K)	$\alpha_{VG}$ (kPa <sup>-1</sup> )	$n_{VG}$ (-)
Bonny silt	-0.516	298.15	0.330	1.61
Bourke silt			0.021	1.54
Completely decomposed tuff			0.023	1.46

743

744

745

746

**Table 2.** Index and compaction properties of Bonny silt (after Alsherif and McCartney, 2015)

Property (unit)	Magnitude
Liquid limit (%)	25
Plastic limit (%)	21
Specific gravity	2.65
Maximum dry unit weight (kN/m <sup>3</sup> )	16.3
Initial void ratio	0.68
Optimum moisture content (%)	13.6

747

748

749

750

751

752

753



754  
755

**Table 3.** Experimental tests from the literature used for calibration and validation

Soil Type	Reference	Net Normal Stress (kPa)	Temperature (°C)	Suction (kPa)
Bourke silt	Uchaipichat and Khalili (2009)	150	25	100
				300
			40	100
				300
			60	100
				300
Completely decomposed tuff	Zhou et al. (2015)	200	20	1
				150
			60	1
				150

756

757

758

759

760

**Table 4.** Calibrated fitting parameters for the proposed shear modulus model at ambient temperature.

Soil Type	$n$	$A$	$K_{ref}$
Bourke silt	0.35	40	1.3
Completely decomposed tuff	0.95	220	0.5

761

762

763

764

765

766 **Table A1.** Enthalpies of immersion per unit area of different materials reported in the literature

Material	<i>T</i> of observation (°C)	$\Delta h$ (mJ/ m <sup>2</sup> )	Reference
Silica	35	-195	Khalil (1978)
	35	-202	Khalil (1978)
	35	-278	Khalil (1978)
	35	-309	Khalil (1978)
Quartz	31	-505	Partyka et al. (1979)
	31	-510	Partyka et al. (1979)
	25	-120	Whalen (1961)
	25	-120	Whalen (1961)
Anatase (untreated)	25	-510	Harkins and Jura (1944)
Anatase (coated with Al <sub>2</sub> O <sub>3</sub> )	25	-630	Harkins and Jura (1944)
Na-bentonite	20	-400	Kahr et al. (1990)
Ca-bentonite	20	-750	Kahr et al. (1990)
Plano silt loam	25	-516	Grant and Salehzadeh (1996)
Elkmound sandy loam	25	-285	Grant and Salehzadeh (1996)
Kaolinite	25	-358	Brooks (1960)
Bentonite	25	-575	Zettlemoyer et al. (1955)

767

768

769

770

771

772

773

774

775

776

777 **LIST OF FIGURES:**

778 **Fig. 1.** Temperature effects on: (a) surface tension, (b) enthalpy of immersion with different values  
779 at the reference temperature, (c) contact angle at different values of enthalpy of immersion  
780 at the reference temperature, and (d) matric suction for various pore sizes.

781 **Fig. 2.** Comparison of predicted versus measured effective saturation for Bonny silt at  $T = 23^{\circ}\text{C}$   
782 and  $64^{\circ}\text{C}$  (measured data from Alsherif and McCartney, 2015).

783 **Fig. 3.** Effective saturation versus matric suction at different soil temperatures using the extended  
784 van Genuchten SWRC model: (a) Bonny silt, (b) Bourke silt, and (c) Completely  
785 decomposed tuff.

786 **Fig. 4.** Schematic diagram showing the experimental setup.

787 **Fig. 5.** Measured and proposed variation in small strain shear modulus with matric suction at  $T =$   
788  $23^{\circ}\text{C}$  (with calibrated model values) and  $43^{\circ}\text{C}$  (with predicted model values).

789 **Fig. 6.** Measured shear moduli versus shear strain for completely decomposed tuff reported by  
790 Zhou et al. (2015) and best fit curves through the measured data.

791 **Fig. 7.** Comparison of inferred shear modulus at 0.001% strain ( $G_{0.001}$ ) with calibrated shear  
792 modulus at ambient temperature and predicted shear modulus at elevated temperatures.

793  
794

795

796

797

Figure 1

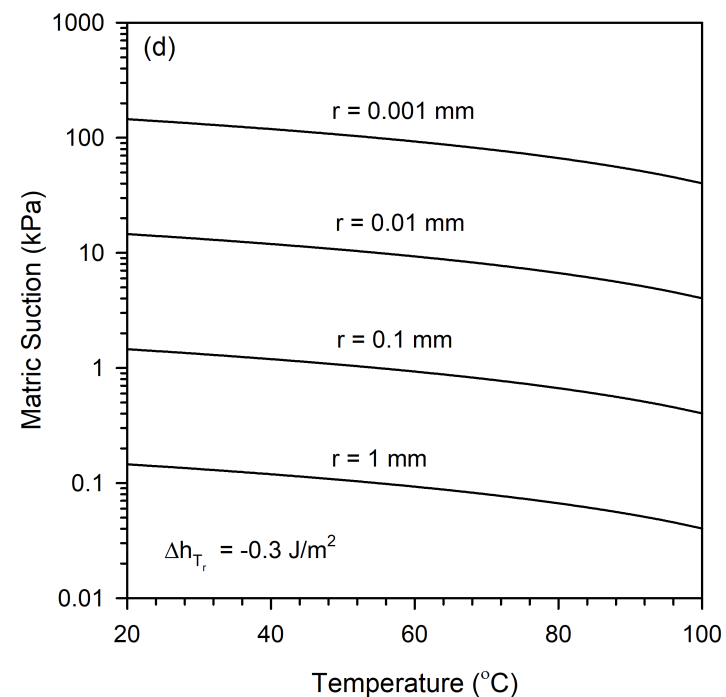
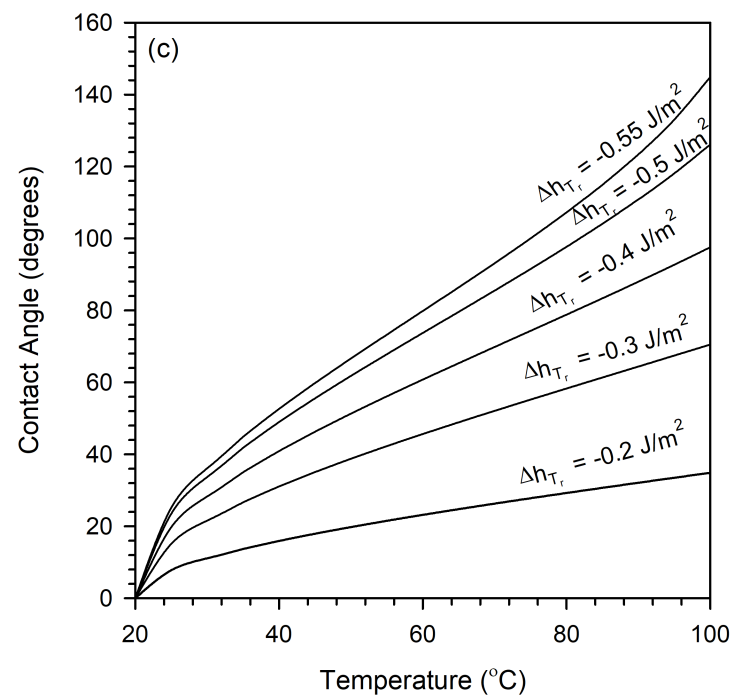
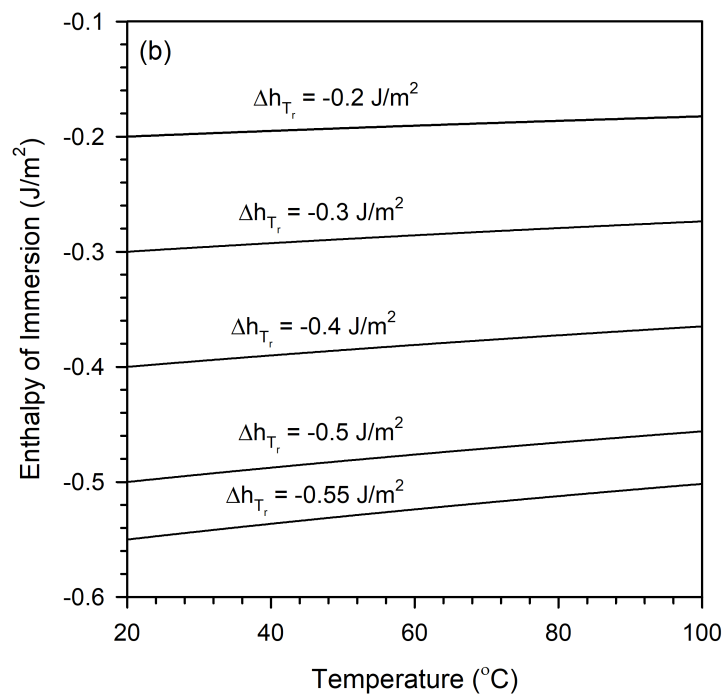
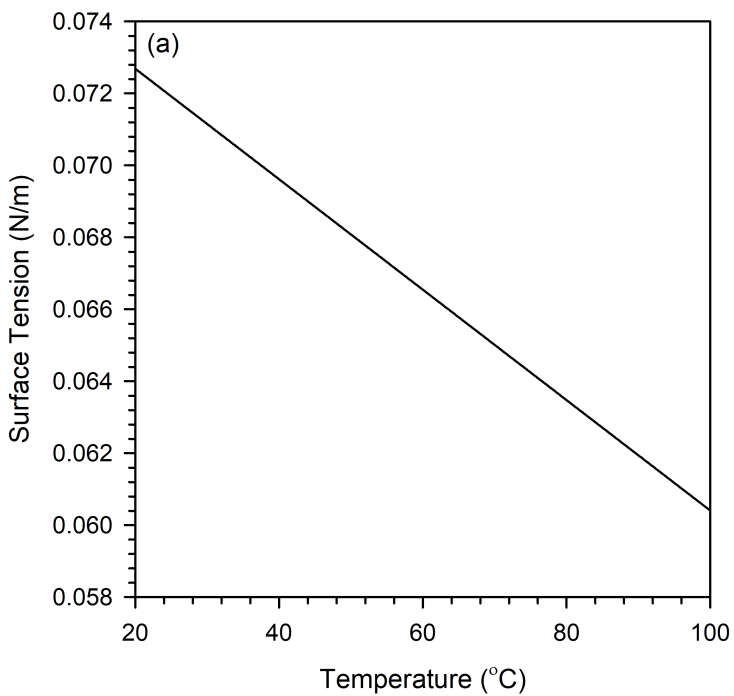


Figure 2

[Click here to access/download;Figure;Fig.2.](#)

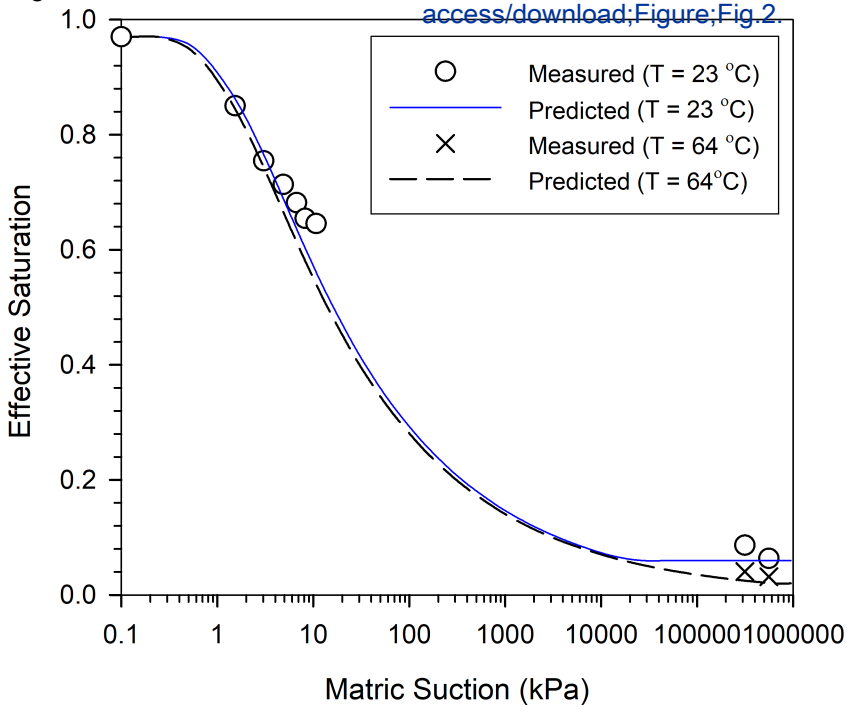
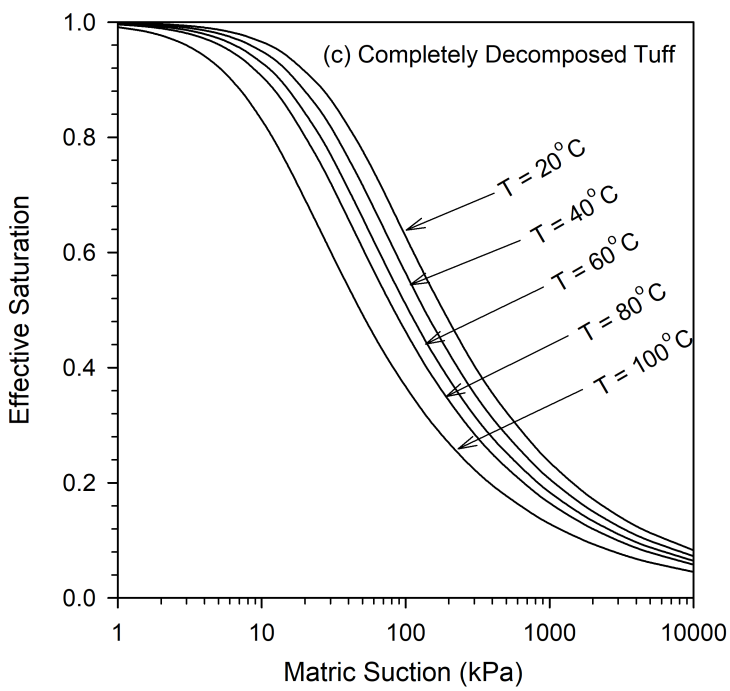
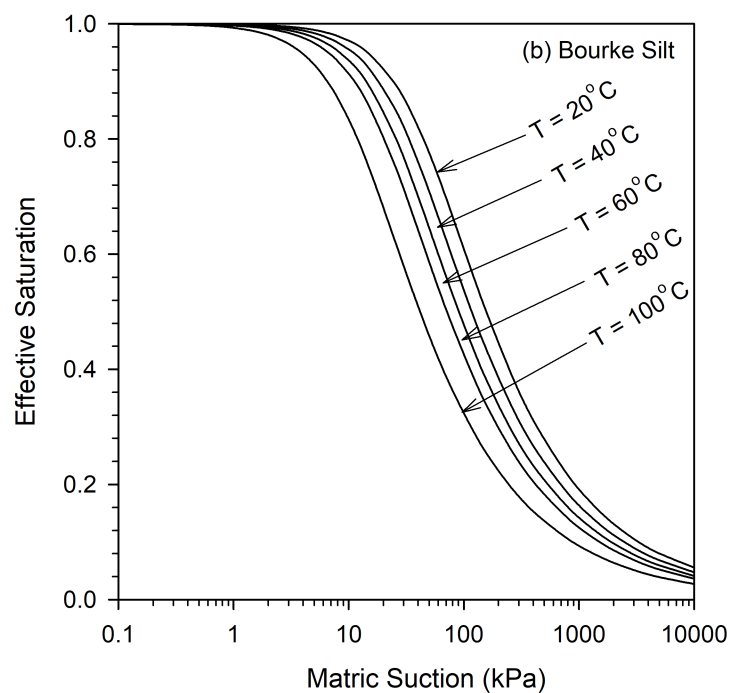
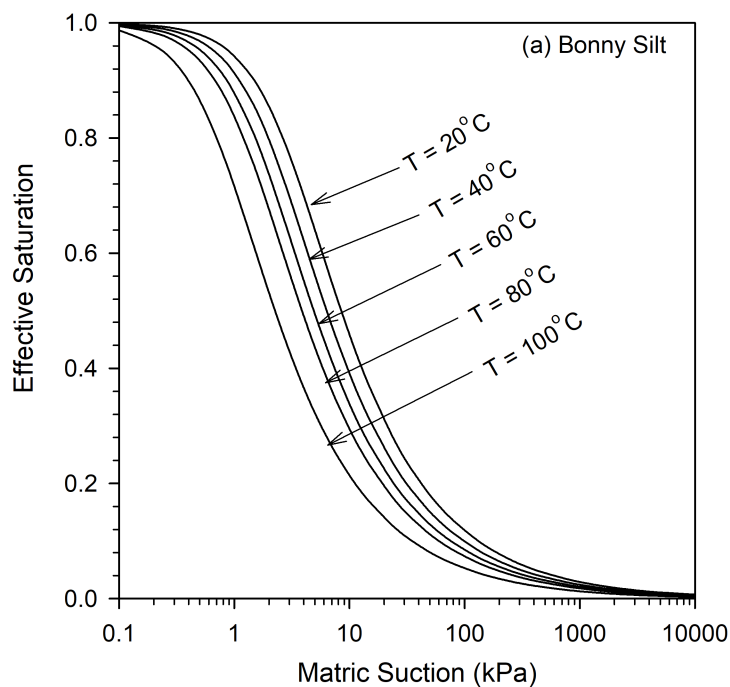


Figure 3

[Click here to access/download;Figure;Fi](#)

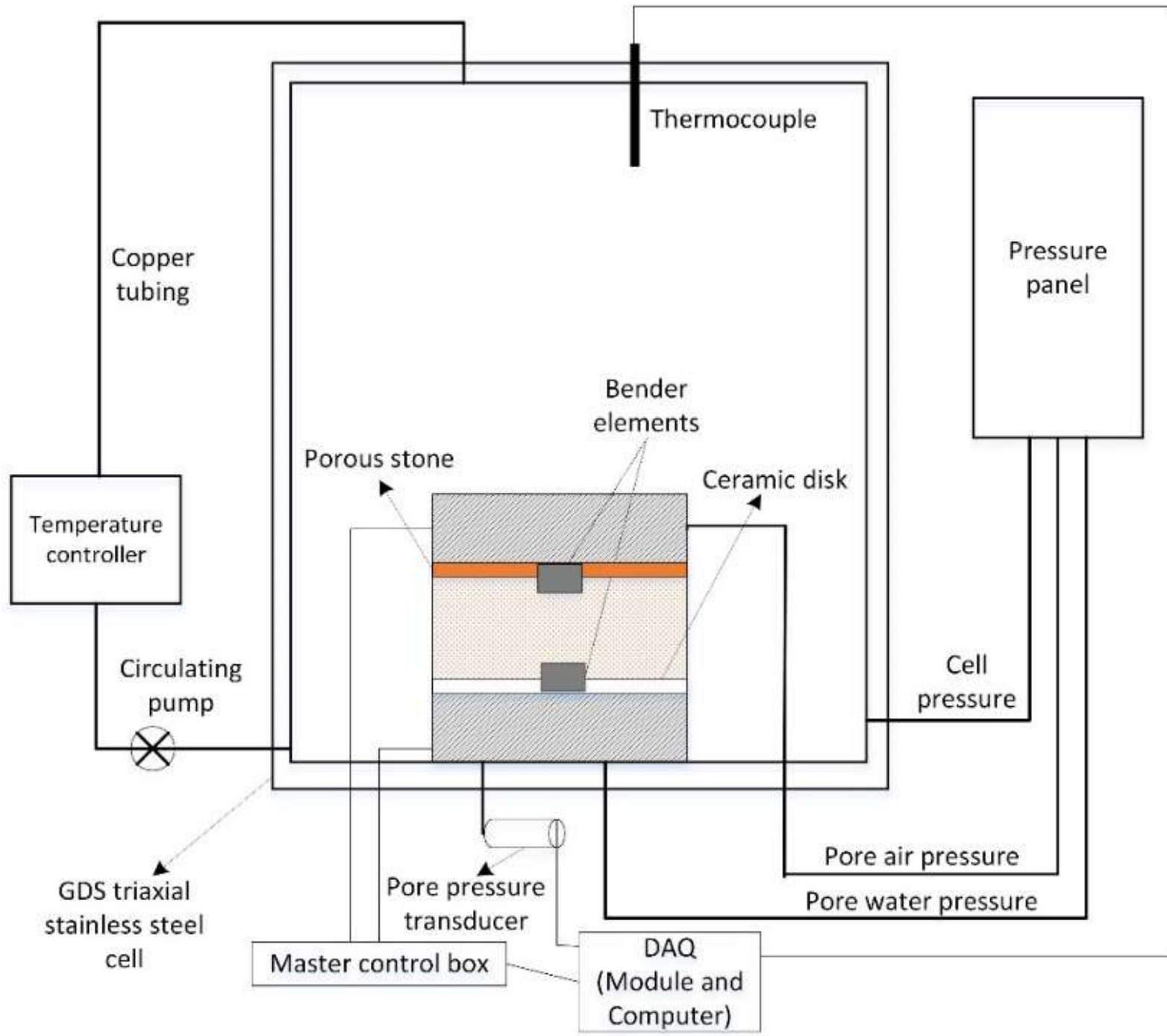
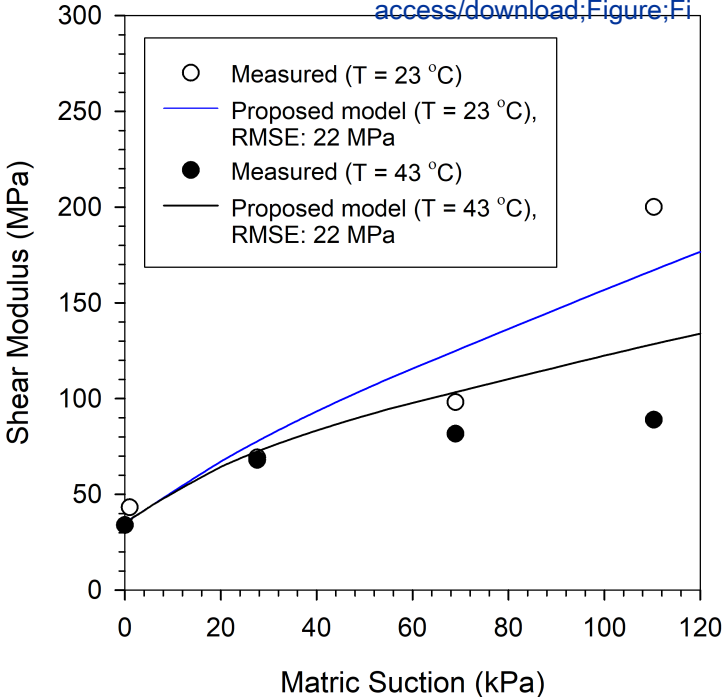


Figure 5

[Click here to access/download;Figure;Fi](#)





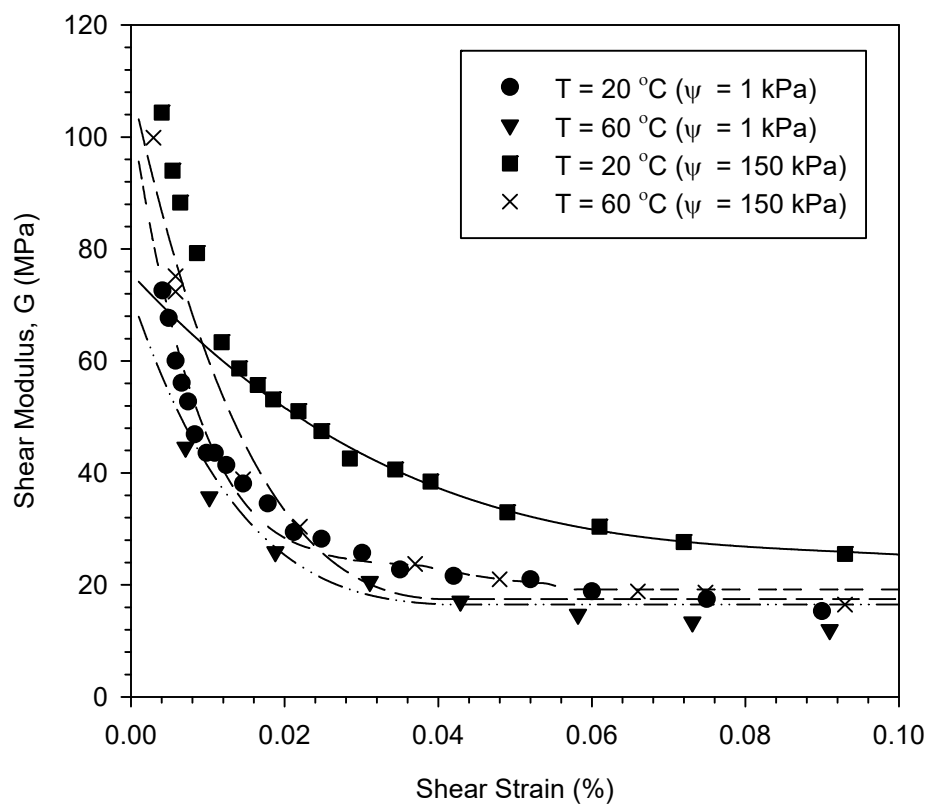
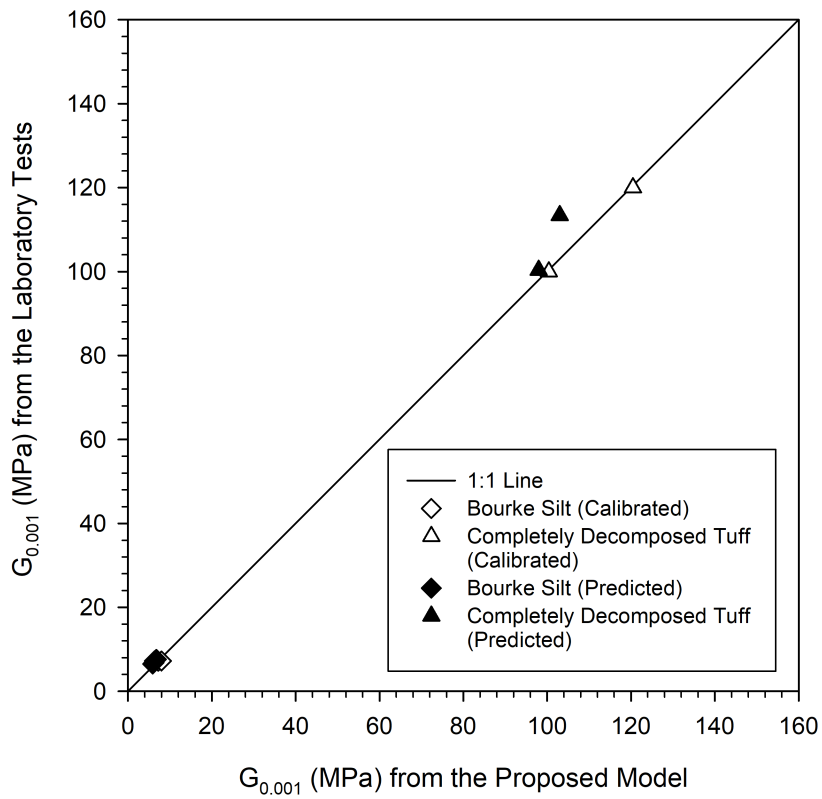


Figure 7



## **Response to Review Comments by Reviewer #2 (Manuscript MS GTENG-8804)**

This manuscript is a major revision of a previous submission to JGGE. The major comments from this reviewer have been addressed.

**Response/Change:** We thank the reviewer for taking the time to review our new submission. We are glad to hear the reviewer found our changes and responses to the comments satisfactory. Please see below for our itemized response, and associated changes made in the revised manuscript.

The only minor issue is that the descriptions about Fig. 6 are confusing. Please clarify: are the lines in this figure produced by the proposed closed-form model using one set of parameters? or each curve uses a different set of parameters? If the former, please present the parameters. If it is the latter, there is not much point to show Fig.6 because one may just fit it with a Hardin's equation as well.

**Response/Change:** We didn't use our proposed model to generate curves shown on Fig. 6. Our proposed equation is for small strains ( $<0.001\%$ ), where the shear modulus is strain independent. Fig. 6 shows the measured values of shear modulus at different strain levels from Zhou et al. (2015). They reported shear modulus values for strain levels of 0.003% to 1%. However, to compare their results against our model at small strains ( $<0.001\%$ ), we fitted each of their measured data set with a polynomial function and then extrapolated to infer the "measured" values at small strains (i.e.,  $<0.001\%$ ) using their data. The measured small strain shear modulus values obtained after extrapolation are compared against the "predicted" values from our proposed equation (see Fig. 7). We clarified this aspect in the paper.